International Journal of Pharmaceutics 384 (2010) 154–164

Contents lists available at ScienceDirect

International Journal of Pharmaceutics

journal homepage: www.elsevier.com/locate/ijpharm

Pharmaceutical Nanotechnology

Nanoparticles formed from PNIPAM-*g*-PEO copolymers in the presence of indomethacin

V. Michailova[a,*], I. Berlinova[b], P. Iliev[b], L. Ivanov[a], S. Titeva[a], G. Momekov[a], I. Dimitrov[b]

[a] *Faculty of Pharmacy, Medical University of Sofia, Sofia 1000, Bulgaria*
[b] *Institute of Polymers, Bulgarian Academy of Sciences, Sofia 1113, Bulgaria*

ARTICLE INFO

Article history:
Received 11 June 2009
Received in revised form
16 September 2009
Accepted 18 September 2009
Available online 25 September 2009

Keywords:
Double-hydrophilic graft copolymers
Poly(*N*-isopropylacrylamide)-*g*-poly(ethylene oxide)
Cononsolvency
Nanoparticles
Indomethacin
Drug release

ABSTRACT

Biocompatible double-hydrophilic PNIPAM-*g*-PEO copolymers containing 0.3–3.2 mol% PEO grafts were synthesized and utilized to prepare indomethacin (IMC)-loaded core–shell nanoparticles by dialysis and nanoprecipitation methods. IMC loading was conducted at room temperature using the organic solvents ethanol and DMF, which induced phase separation in the copolymers aqueous solutions due to the cononsolvency of PNIPAM. In ethanol–water solutions, the cononsolvency-induced phase separation of the copolymers promoted effective drug incorporation into the formed micellar structures. In DMF–water system, the formation of the nanoparticles did not correspond to the cononsolvent region of PNIPAM-*g*-PEO. In this case, hydrophobic interactions between PNIPAM and IMC allowed the copolymer self-association and drug loading. Irrespective of the solvents or preparation methods applied, the drug loading content (DLC) depended on the drug-to-copolymer feed weight ratio. DLC was relatively low at the 0.5:1 ratio but it significantly increased at the ratios of 0.75:1 and 1:1 (DLC∼90%). The particle size was strongly affected by the different mechanisms of nanoparticles formation. The nanoprecipitation from ethanol produced significantly smaller particles (<150 nm) with narrow size distribution than the dialysis from DMF. The velocity of indomethacin release from the nanoparticles was influenced by the amount of encapsulated drug, the process being faster at lower DLC.

1. Introduction

In the recent years, polymeric micelles with core–shell morphology have attracted much attention for their potential application in drug delivery (Allen et al., 1999; Kataoka et al., 2001; Gaucher et al., 2005; Torchilin, 2007; Bromberg, 2008). Particles with nanometer-scale dimensions, obtained by self-assembly of amphiphilic or double-hydrophilic block copolymers are of interest as carriers that can entrap mainly hydrophobic and poorly water-soluble drugs through hydrophobic, hydrogen-bonding, or electrostatic interactions. The small size, appropriate surface properties, and enhanced stability of the loaded nanoparticles ensure their prolonged circulation in the blood and access to diseased organs, tissues or cells (Bae and Kataoka, 2005). The pharmacokinetics of the entrapped drugs can be modulated by changing the polymer architecture and characteristics of the core-forming blocks as well as by the incorporation of a thermo-responsive polymeric segment in either the micellar core or corona (Rösler et al., 2001; Qiu and Bae, 2006). The conversion of the thermally sensitive component from hydrophobic to a more hydrophilic state or vice versa in response to small changes in temperature permits temporal and spatial delivery control of the incorporated drug (Rijcken et al., 2007).

Temperature responsive polymers like poly(*N*-isopropylacrylamide) (PNIPAM) homopolymer and its copolymers have been widely applied for the formation of thermo-sensitive drug delivery systems because they exhibit reversible phase transition in water around body temperature, the lower critical solution temperature (LCST). Additives such as salts, proteins, low molecular drugs and some polar organic solvents affect significantly their critical temperature by changing the hydrophilic/hydrophobic balance within the polymer molecule via different mechanisms of hydration or dehydration (Eeckman et al., 2001; Costa and Freitas, 2002; Liu et al., 2004; Chaw et al., 2004; Coughlan and Corrigan, 2006). For example, hydrophobic drugs like benzoic acid and its derivatives as well as ibuprofen associate with PNIPAM by hydrophobic interactions and hydrogen-bonding which results in a more hydrophobic system and a concomitant decrease in the phase transition temperature. Such drug-induced changes in the thermal sensitivity of PNIPAM have been found to impact on the equilibrium swelling degree and drug release rate of PNIPAM hydrogel matrices (Lowe and Tenhu, 1998; Coughlan et al., 2004; Coughlan and Corrigan, 2008).

* Corresponding author at: Department of Pharmaceutical Technology and Biopharmacy, Faculty of Pharmacy, Medical University of Sofia, 2 Dunav Street, Sofia 1000, Bulgaria. Tel.: +359 2 9236 546; fax: +359 2 9879874.
E-mail address: vmihailova@pharmfac.acad.bg (V. Michailova).

0378-5173/$ – see front matter © 2009 Elsevier B.V. All rights reserved.
doi:10.1016/j.ijpharm.2009.09.034

Double-hydrophilic graft copolymers PNIPAM-*g*-poly(ethylene oxide) (PNIPAM-*g*-PEO) composed of a PNIPAM backbone and PEO side chains, exhibit LCST around that of PNIPAM homopolymers or higher, depending on the number and distribution of the grafted PEO, the length of the PNIPAM backbone and the copolymer concentration (Virtanen and Tenhu, 2000; Bisht et al., 2005). Below the LCST, these copolymers readily dissolve in water; at temperatures above the critical point, they self-assemble into single chain or inter-chain nanostructures consisting of a collapsed PNIPAM inner core and a hydrated PEO outer shell, which confers colloidal stability to the system. The degree of interchain aggregation and the nanoparticles size are mostly determined by the competition between the hydrophobic interactions in PNIPAM and the solubilizing and surface stabilization effect of PEO on the shrinking backbone. Some technological factors such as the rate of heating and the copolymer concentration can also affect the nanoparticles size by the change in the balance between intrachain contraction and interchain association of PNIPAM as well as by the resulting viscoelasic effects (Qiu and Wu, 1997; Virtanen et al., 2000; Chen et al., 2005).

The PNIPAM-*g*-PEO core–shell nanoparticles have not been employed so far in drug delivery applications, yet, their ability to solubilize small amounts of lipophilic and amphiphilic probe molecules upon heating at T > LCST and to dissolve and release the probe at room temperature has been proved by fluorescence and EPR spectroscopy studies (Wu and Qiu, 1998; Virtanen et al., 2001). In this work, we evaluated the capacity of double-hydrophilic PNIPAM-*g*-PEO copolymers containing 0.3–3.2 mol% PEO grafts to incorporate and retain indomethacin inside the hydrophobic inner core of the micellar nanoparticles formed at T < LCST of the copolymers. Indomethacin was selected as a model drug because of its specific chemical structure and physicochemical properties (e.g., H-bonding carboxylic acid group, hydrophobic nature, pH-dependent solubility) that were expected to affect the processes of nanoparticles formation and loading as well as the drug release rate.

2. Materials and methods

2.1. Materials

α-Methoxy-ω-hydroxy-polyoxyethylene (MPEO) with M_n = 2000 was purchased from Fluka. Indomethacin (IMC, 1-(4-chlorobenzoyl)-5-methoxy-2-methyl-1*H*-indole-3-acetic acid) and the other reagent grade chemicals were Aldrich products. *N*-isopropylacrylamide (NIPAM) was recrystallized from a 65:35 (v/v) mixture of hexane and benzene. Maleic anhydride was recrystallized from benzene. Azobisisobutyronitrile (AIBN) was purified by recrystallization from methanol. *N*-hydroxyphthalimide, *N*,*N*′-dicyclohexylcarbodiimide (DCC), and morpholine were used as received. Solvents such as diethyl ether, methylene chloride, toluene, benzene and hexane were dried prior to use. Dimethylformamide (DMF) and 95% ethanol were used for IMC and graft copolymers dissolution.

2.2. Synthesis and characterization of PNIPAM-g-PEO copolymers

2.2.1. Synthesis of MPEO monoester of maleic acid (MEMA)

MEMA was prepared through the reaction of MPEO with maleic anhydride. In a typical reaction, MPEO (10 g, 5 mmol), maleic anhydride (3 g, 30 mmol) and toluene (40 ml) were placed in a reaction vessel and the mixture was heated at 80 °C for 48 h. Then the solvent was removed, the residue was dissolved in methylene chloride, and precipitated into large excess of anhydrous diethyl ether. Yield: 9.9 g, 95%. ^{1}H NMR ($CDCl_3$, δ): 6.4, 6.2 (d, 1H and d, 1H, HOOC-C*H*=C*H*-COOR); 4.36 (t, 2H, CH_2CH_2-OC(O)); 3.67 (t, 182 H, O-CH_2CH_2-O); 3.37 (t, 3H, O-CH_3).

2.2.2. Synthesis of MPEO phthalimido maleate (MEPAM)

MEMA (1.05 g, 0.5 mmol) and *N*-hydroxyphthalimide (0.081 g, 0.5 mmol) were dissolved in 10 ml of methylene chloride. DCC (0.105 g, 0.5 mmol) dissolved in 2 ml of methylene chloride was added and the reaction mixture was stirred for 20 h. The mixture was filtered and the polymer precipitated into diethyl ether. Yield: 1 g, 88%. ^{1}H NMR ($CDCl_3$, δ): 7.73 (4H, C(O)C_6H_4C(O)); 6.4, 6.2 (d, 1H and d, 1H, HOOC-C*H*=C*H*-COOR); 4.36 (t, 2H, CH_2CH_2-OC(O)); 3.67 (t, 182 H, O-CH_2CH_2-O); 3.37 (t, 3H, O-CH_3).

2.2.3. Synthesis of PNIPAM-g-PEO copolymers

PNIPAM-*g*-PEO copolymers were obtained by radical copolymerization of MEPAM macromonomer with NIPAM in benzene in the presence of morpholine. The molar content of the macromonomer in the feed varied in the range of 0.5–5 mol%. In a typical procedure, 0.52 g of MEPAM, 1.28 g of NIPAM, 0.038 g of AIBN and 0.03 ml of morpholine were dissolved in 10 ml of benzene. The copolymerization was carried out in sealed ampoules under high vacuum at 60 °C for two days. Then the reaction mixture was diluted with methylene chloride and precipitated into diethyl ether. An aqueous solution of the polymer was dialyzed (Spectra/Por membrane tubing, MWCO 12,000) against distilled water for 14 days. The graft copolymer was recovered by lyophilization.

The composition of the graft copolymers was determined by ^{1}H NMR in $CDCl_3$. The relative intensities of the signals of the oxyethylene protons at δ 3.67 and of methyl protons at δ 1.12 enabled the estimation of the approximate number of NIPAM units (y) per grafted PEO chain (Eq. (1)),

$$\frac{\text{Area of PNIPAM protons at } \delta\, 1.12}{\text{Area of PEO protons at } \delta\, 3.67} = \frac{6y}{4n(\text{PEO})} \quad (1)$$

where n is the degree of polymerization of PEO.

The copolymerization products were denoted *x*PNEM, where *x* stands for the molar content of the PEO macromonomer in the purified graft copolymer.

2.3. Structural characterization of copolymers

^{1}H NMR spectra were recorded on Bruker 250 MHz spectrometer in $CDCl_3$ at 20 °C. Size exclusion chromatography (SEC) measurements were performed on a system (Waters Associates, USA) consisting of a M510 pump, a U6K injector, refractometer 410, and a set of 10 μm mixed-B, and 5 μm 100 Å PL gel columns. The mobile phase was THF at a flow rate of 1 ml/min at 45 °C. The weight average molecular weight, M_w, of copolymers was determined by static light scattering (SLS). SLS measurements were carried out on a multi-angle DAWN DSP Laser light scattering photometer (Wyatt Technology Corp., USA) equipped with a He-Ne laser emitting at a wavelength of 632.8 nm. Analyses were performed in a batch mode. Specific refractive index increments, dn/dc, were measured on a Wyatt Optilab 903 interferometric refractometer operating at 633 nm. The stock solutions for the light scattering measurements were prepared at concentration of 3×10^{-3} g/ml. They were purified of dust using filter of 0.2 μm pore size (PVDF filter) and diluted with filtered solvent.

2.4. In vitro study of copolymers biocompatibility

2.4.1. Cell culture conditions

The human embryonal kidney cell line HEK-293 was purchased from the German Collection of Microorganisms and Cell Cultures (DSMZ GmbH, Braunschweig, Germany). They were cultured under standard conditions—RPMI-1640 medium supplemented with 10%

fetal bovine serum and 2 mM L-glutamine, at 37 °C in an incubator with humidified atmosphere and 5% CO_2.

2.4.2. In vitro biocompatibility assessment (MTT-dye reduction assay)

Stock solutions of the copolymers were freshly prepared in DMSO and consequently diluted with RPMI-1640 medium to yield the desired final concentrations (at the final dilution, the concentration of the solvent never exceeded 1%). The cell viability was assessed using the standard MTT-dye reduction assay (Mosmann, 1983), with minor modifications (Konstantinov et al., 1999). The cells were seeded in 96-well microplates (100 μl/well) at a density of 1×10^5 cells per ml and after 24 h incubation at 37 °C they were exposed to various concentrations (0.125–2 mg/ml) of the copolymers for 72 h. For each concentration at least 8 wells were used. After the incubation, 10 μl of the MTT solution (10 mg/ml in PBS) were added to each well. The microplates were further incubated for 4 h at 37 °C and the formed MTT-formazan crystals were dissolved by adding 100 μl per well of a 5% HCHO solution in 2-propanol. The MTT-formazan absorption was determined using a microplate reader (Labexim LMR-1) at 580 nm.

2.4.3. Data processing and statistics

The cell survival data were normalized as percentage of the untreated control (set as 100% viability). The statistical processing of biological data included the Student's *t*-test whereby values of $p \leq 0.05$ were considered as statistically significant.

2.5. Phase transition measurements

2.5.1. Cloud point determination

The cloud points (CPs) for 0.1 wt% solutions of the graft copolymers in water or in a phosphate buffer solution (PBS, pH 7.4) were determined by observing light transmittance. The sample cell was thermostated with a circulating water jacket from 25 °C to 55 °C. The temperature was gradually increased with a heating rate of 0.2 °C/min. The cloud point was defined as the temperature corresponding to a decrease of 10% of the solution transmittance at 500 nm (Boutris et al., 1997).

2.5.2. Phase transition of PNIPAM-g-PEO copolymer in an organic solvent–water mixture

The phase transition of PNIPAM-*g*-PEO copolymer alone and in the presence of IMC was studied in ethanol–water and DMF–water binary mixtures at 20 °C using a spectroscopic technique (Causse et al., 2006). Stock solutions of PNIPAM-*g*-PEO copolymer or of a 1:1 (w/w) IMC-copolymer mixture were prepared in the relevant organic solvent at a polymer concentration of 0.25 wt%. Their optical transmittance was monitored (Hewlett Packard 8452A spectrophotometer) as a function of the solvent-to-water volume ratios at 500 nm upon stepwise addition of small aliquots (250 μl) of water. After the addition of each water portion, the sample was kept under stirring for 20 min to stabilize before the transmittance measuring. The phase separation of 0.25 wt% IMC solutions in ethanol or DMF was also monitored under the same experimental conditions.

2.6. IMC-PNIPAM-g-PEO copolymer interactions studies

The hydrogen-bonding and hydrophobic interactions between IMC and the copolymer were examined by IR and ^{1}H NMR spectroscopy.

2.6.1. IR spectroscopy

The IR spectra were recorded on Bruker Vector 22 spectrometer. Thin films for spectral measurements were prepared by dissolving PNIPAM-*g*-PEO, IMC or an appropriate amount of PNIPAM-*g*-PEO and IMC in ethanol and then several drops of the sample solution were placed onto KBr plates. The plates were dried under vacuum at room temperature.

2.6.2. ^{1}H NMR spectroscopy

^{1}H NMR spectra of IMC-loaded nanoparticles and the respective PNIPAM-*g*-PEO copolymer were performed in D_2O at 20 °C. The spectrum of IMC was recorded at the same temperature, using NaOD/D_2O as a solvent.

2.7. Preparation of IMC-loaded PNIPAM-g-PEO nanoparticles

PNIPAM-*g*-PEO nanoparticles containing IMC were prepared by both the dialysis method (Allen et al., 1999) and the nanoprecipitation technique (Fessi et al., 1989; Bilati et al., 2005). All steps of the two preparation methods employed were conducted at room temperature.

2.7.1. Dialysis method

PNIPAM-*g*-PEO copolymer (50 mg) and IMC (25 mg, 37.5 mg or 50 mg) (copolymer: IMC, 0.5:1, 0.75:1 or 1:1 w/w) were dissolved in 5 ml of DMF or ethanol and the solution was dialyzed against 1000 ml of distilled water for 24 h using a cellulose dialysis membrane with a molecular weight cut-off of 12,000 (Sigma–Aldrich, Germany) at 20 °C. During the first 3 h, water was exchanged every hour and then on the next day. After the dialysis, the colloidal dispersion was filtered through 1.2 μm membrane filter (Whatman GF/Cw/GMF, USA) to remove insoluble material and the filtrate was analyzed or freeze dried for 24 h before further examinations. Each experiment was performed in triplicate.

2.7.2. Nanoprecipitation method

PNIPAM-*g*-PEO copolymer (50 mg) and IMC (25 mg, 37.5 mg or 50 mg) (copolymer: IMC, 0.5:1, 0.75:1 or 1:1, w/w) were dissolved in 5 ml of ethanol. Then the solution was slowly injected into 95 ml of distilled water under moderate magnetic stirring. The resulting opalescent solution was allowed to stir for 10 min at room temperature. Afterwards, it was dialyzed against water for 6 h to remove the organic solvent and filtered through 0.80 μm membrane filter (Sartorius AG, Germany). The loaded nanoparticles were recovered by freeze drying for 24 h. Each experiment was performed in triplicate.

2.8. Characterization of IMC-loaded nanoparticles

2.8.1. Particle size measurement

The average size and size distribution of the nanoparticles were estimated by dynamic light scattering (DLS) using a Malvern Zetasizer Nano 3600 (Malvern Instruments Ltd., UK) equipped with a He-Ne laser (0.4 mW; 633 nm) and a temperature-controlled cell holder. The intensity of the scattered light was detected at 90° to the incident beam. The nanoparticles dispersions were prepared by the above described methods and were analyzed at 20 °C and 37 °C, at a sample concentration of 0.2 mg/ml. The particle size was measured starting at 20 °C. Then, the temperature of the samples was increased to 37 °C in 45 min and the particle size was determined by DLS after equilibration of 30 min. The mean intensity-weighted diameter was recorded as the average of three measurements.

2.8.2. Scanning electron microscopy (SEM)

SEM observations were conducted on a JEOL JSM-5510 (JEOL, Japan) at 10 kV. The specimens for SEM observations were prepared by spin casting the sample solution in water on a clean glass slide. All the glass slides used were first washed with distilled water and then with acetone. A thin layer of gold was sputter-coated on the

samples with the aid of JEOL JFC-1200 fine coater (JEOL, Japan) for charge dissipation during SEM imaging.

2.8.3. Determination of drug loading content and entrapment efficiency

The IMC loading was quantified using a high-performance liquid chromatographic (HPLC) assay (Hewlett Packard 1040 M) after dissolution of the freeze-dried nanoparticles in an appropriate amount of the mobile phase. The chromatographic procedure was carried out at 20 °C using a reverse-phase C_{18} column (Kromasil 100-5 C_{18}, 125 × 4 mm, 5 μm), acetonitrile–water (0.1% TFA) 80:20 as a mobile phase with a flow rate of 1 ml/min, and a detection wavelength of 320 nm (Djordjevic et al., 2005). The IMC concentration in the samples was obtained from a calibration curve. The drug loading content (DLC) and entrapment efficiency (EE) of the IMC-loaded nanoparticles were calculated according to Eqs. (2) and (3):

$$\mathrm{DLC\,(wt\%)} = \frac{\text{the amount of IMC in nanoparticles}}{\text{the amount of polymer added initially}} \times 100 \quad (2)$$

$$\mathrm{EE\,(w/w_p\%)} = \frac{\text{the total amount of IMC in nanoparticles}}{\text{the amount of IMC added initially}} \times 100. \quad (3)$$

2.9. In vitro IMC release studies

In vitro release studies were conducted in acetate buffer solution (pH 4.5) and in phosphate buffer solution (0.06 mol/l, pH 7.4) using the dialysis tube method (D'Souza and DeLuca, 2006). In a typical experiment, 7 mg of lyophilized IMC-loaded nanoparticles were dispersed in 5 ml of the respective buffer solution at room temperature. Then the dispersion was transferred into a dialysis tube closed at one end with a dialysis membrane (7.065 cm^2 exposed area, MWCO 12,000–14,000, Sigma–Aldrich, Germany). The dialysis tube was then immersed into an outer vessel containing 150 ml of the buffer solution. During the experiment, the temperature of the entire assembly was maintained at 37 °C ± 0.5 °C, using a circulating water jacket. At appropriate intervals, 3-ml aliquots were withdrawn from the outer aqueous solution and replaced with an equal volume of the fresh release medium. The released IMC was quantified by UV spectroscopy (Hewlett Packard 8452A) at 320 nm, using a standard calibration curve. Each *in vitro* release experiment was repeated four times.

3. Results and discussion

3.1. Synthesis and characterization of PEO macromonomer and PNIPAM-g-PEO copolymers

The synthesis of the double-hydrophilic PNIPAM-*g*-PEO copolymers consists of three consecutive steps: (1) synthesis of MPEO monoester of maleic acid (MEMA), (2) its esterification with *N*-hydroxyphthalimide to obtain MPEO phthalimido maleate, and (3) copolymerization of MEPAM macromonomer with NIPAM.

The interaction of MPEO with maleic anhydride proceeded quantitatively in toluene at 80 °C. The esterification of the resulting MPEO monoester of maleic acid with *N*-hydroxyphthalimide produced the corresponding diester of maleic acid, MEPAM. The phthalimido esters are activated carboxylic ester units that readily react with amines and provide a possibility of affecting the phase and conformational behavior of the double-hydrophilic graft copolymers. The structure of the activated ester was confirmed by the ^{1}H NMR spectrum in $CDCl_3$ (Fig. 1). The ratio of the intensities of the phthalimide protons at 7.73 ppm, the CH_2 protons adjacent

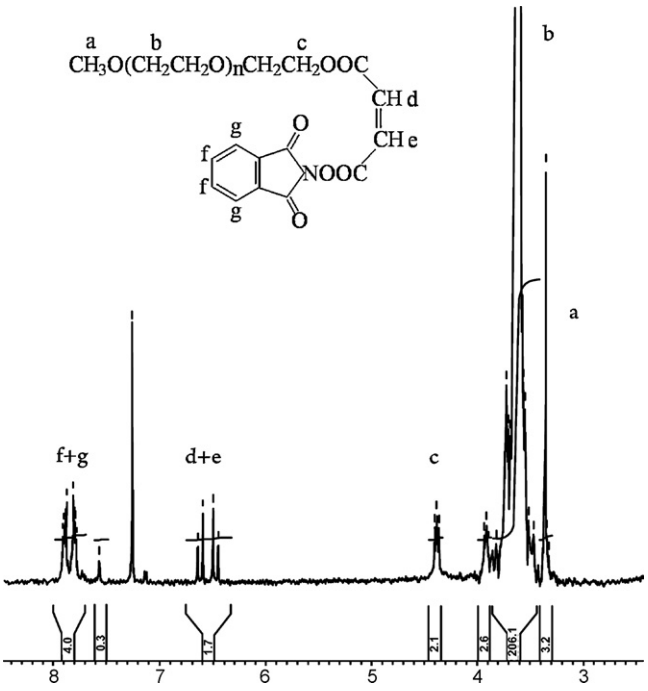

Fig. 1. ^{1}H NMR spectrum of MPEO phthalimido maleate in $CDCl_3$.

to the ester group at 4.36 ppm and the C*H*=C*H* protons at 6.4 ppm and 6.2 ppm was found to be 4:2:2.

The graft copolymers were obtained by the "grafting through" method (Fig. 2). To enhance the reactivity of the maleic acid macromonomer derivatives, the copolymerization was performed in the presence of morpholine as an isomerization catalyst (Otsu et al., 1981). Since morpholine is a secondary amine, the phtalimido groups were substituted with morpholine groups to yield the copolymer *x*PNEM. These groups were not expected to have implications for PNEM biocompatibility since polymers containing morpholine are known as nontoxic materials (Ranucci et al., 1994). The grafting degree of the copolymers obtained was low, in the range of 0.3–3.2 mol%. The characteristics of the graft copolymers are summarized in Table 1. The molecular weights of the graft copolymers were determined by SLS in methanol and the molecular weight distributions were obtained from SEC measurements. The weight average molecular weights (M_w) ranged from 0.9×10^5 to 2.4×10^5. The SEC traces of the graft copolymers were monomodal, lacking traces of macromonomer contamination.

Table 1
Characteristics of PNIPAM-*g*-PEO graft copolymers.

Graft copolymer			PEO grafts		CP (°C)[a]	
Sample[b]	M_w[c] (g mol^{-1})	PDI[d]	mol%	wt%	Aqueous solution	PBS pH 7.4
*0.3*PNEM	2.4×10^5	1.73	0.3	5	32.5	30.9
*1.1*PNEM	2.0×10^5	1.75	1.1	18	35.7	34.2
2.2 PNEM	1.7×10^5	1.66	2.2	30	39.1	35.0
*2.7*PNEM	1.5×10^5	1.65	2.7	35	–[e]	36.8[f]
*3.2*PNEM	0.9×10^5	1.54	3.2	39	–[e]	37.2[f]

[a] Cloud point temperature of a 0.1 wt % solution at 10% loss of transmittance at 500 nm.
[b] The number code indicates the content of PEO grafts (mol%).
[c] Measured by light scattering in methanol.
[d] Polydispersity index.
[e] The transmittance did not decrease upon increasing solution temperature up to 50 °C.
[f] The transmittance was measured at 400 nm.

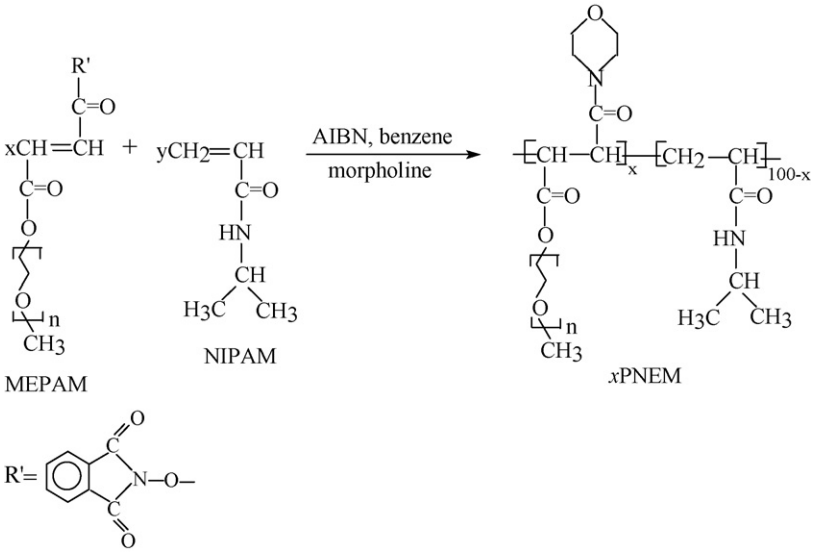

Fig. 2. Synthesis of PNIPAM-*g*-PEO graft copolymers through copolymerization of NIPAM and a poly(oxyethylene) (PEO) macromonomer; *x*—the molar content of the PEO macromonomer in the graft copolymer; $n = 44$.

The CPs for the graft copolymers solutions in water and in pH 7.4 PBS were determined by transmittance measurements (Table 1). In water, the CPs increased with increasing the molar content of the PEO-macromonomer from 0.3 to 2.2 mol%. At higher degree of PEO grafting, phase transition was not observed upon increasing the solution temperature up to 50 °C, which may be ascribed to the significant increase in the hydrophilic properties of the copolymers (Schmaljohann, 2006). In PBS the graft copolymers displayed transition at lower temperatures compared to the pure aqueous solutions. The buffer salts have a "salting out" effect on the PNIPAM segments, similar to salts effect on the phase transition of linear and cross linked PNIPAM (Eeckman et al., 2001; Coughlan and Corrigan, 2006).

Biocompatibility of *1.1*PNEM, *2.2*PNEM and *3.2*PNEM copolymers was evaluated *in vitro* by assessing the viability of HEK-293 cells (MTT-dye reduction assay). As evident from the cell viability data (Fig. 3), all tested polymers proved to be devoid of cytotoxic effects against the tested cell line after 72 h continuous exposure at 37 °C. Only at the highest copolymers concentration (2 mg/ml) there was some, statistically insignificant decrease in the cell viability ($p > 0.05$). These results suggest that the synthesized graft copolymers are biocompatible and, hence, suitable for pharmaceutical application.

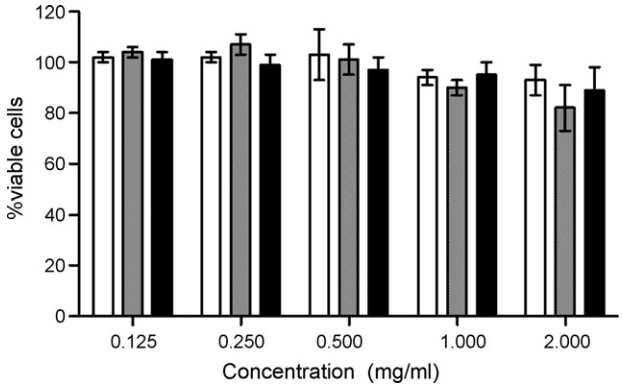

Fig. 3. Cytotoxic effects of PNIPAM-*g*-PEO graft copolymers against a human embryonal kidney cell line HEK-293 after 72 h continuous exposure (MTT-dye reduction assay). *1.1*PNEM (white columns), *2.2*PNEM (grey columns) and *3.2*PNEM (black columns). Each column represents a mean value ± SD of 8 independent experiments.

3.2. Preparation of IMC-loaded PNIPAM-g-PEO nanoparticles

PNIPAM-*g*-PEO nanoparticles were loaded with IMC by the dialysis method and nanoprecipitation technique at 20 °C, using two water-miscible organic solvents, ethanol and DMF. The two solvents were selected because they dissolve both the copolymers and IMC and their mixing with water might induce micellization of PNIPAM-*g*-PEO at room temperature due to the precipitation of PNIPAM segments. Such solvent-induced soluble-insoluble-soluble transition of PNIPAM in mixtures of water with some polar organic solvents like methanol, ethanol, DMSO, THF or DMF, termed cononsolvency, has been related to the competitive interactions among water, the solvent and the polymer, which limit the number of solvents molecules available to solubilize the polymer (Winnik et al., 1993; Tanaka et al., 2009). As the type of interactions between the organic solvent and water depends on the nature of the solvent applied (Costa and Freitas, 2002; Panayiotou et al., 2004), it is expected that the different properties of ethanol and DMF would have implications for the formation and drug loading of the PNIPAM-*g*-PEO nanoparticles.

3.2.1. Phase transition behavior of PNIPAM-g-PEO in mixed water–cononsolvent systems

The cononsolvency of PNIPAM-*g*-PEO copolymer in ethanol–water and DMF–water mixtures was examined at 20 °C in order to avoid the effect of temperature on the phase transition of the copolymer. Stock solutions of *1.1*PNEM in ethanol or DMF were prepared at a concentration of 0.25 wt%. The dependence of the optical transmittance of these solutions on the volume fraction of water, φ_{water}, is shown in Fig. 4. For both organic solvents, the transmittance of the polymer solutions exhibited a minimum around intermediate water concentrations, indicating that the system reversibly changed its dispersing state from molecular to colloidal and back again similar to the conversion of PNIPAM-*block*-PEO copolymers in methanol–water solutions that led to the formation of PNIPAM-core micelles (Rao et al., 2007). The type of the solvent greatly influenced the strength of cononsolvency in PNIPAM-*g*-PEO aqueous solutions. The phase separation was more pronounced and occurred in a wider φ_{water} range in the mixtures of the more hydrophobic ethanol ($0.37 < \varphi_{water} < 0.72$) than in the mixtures of DMF ($0.32 < \varphi_{water} < 0.45$). This effect might be attributed to the predominant type of the solvents hydration,

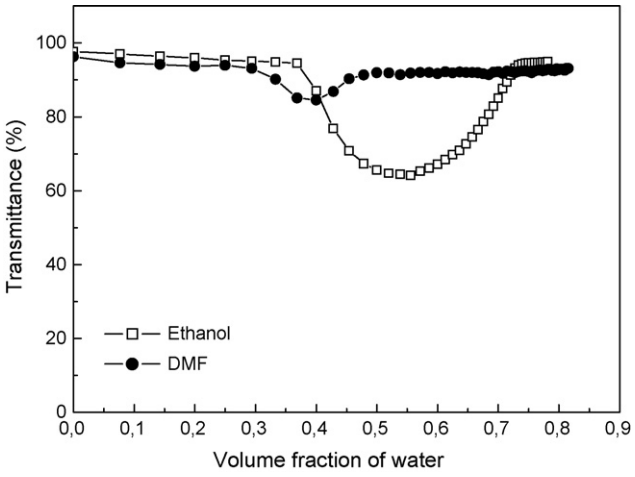

Fig. 4. Optical transmittance of mixed ethanol–water and DMF–water solutions of *1.1*PNEM graft copolymer as a function of the volume fraction of water, at 20 °C.

i.e. H-bonded solvent–water complexes for DMF (Zhu and Napper, 1996a) and hydrophobic hydration for ethanol (Zhu and Napper, 1996b; Costa and Freitas, 2002) that controls the reduction of the number and strength of PNIPAM–water contacts in the region of phase transition.

3.2.2. Phase transition behavior of PNIPAM-g-PEO in mixed water–cononsolvent systems in the presence of indomethacin

The phase transition behavior of PNIPAM-*g*-PEO copolymer in mixed water-cononsolvent systems in the presence of indomethacin was evaluated with *1.1*PNEM-IMC mixture at a drug-to-polymer ratio of 1:1 (w/w), at 20 °C. The changes in the optical transmittance of the *1.1*PNEM-IMC mixture, IMC and the pure *1.1*PNEM in ethanol or DMF solutions as a function of φ_{water} were compared in Fig. 5. In ethanol–water binary solution (Fig. 5a), a rapid and irreversible phase separation was observed in the *1.1*PNEM-IMC mixture, presumably associated with the formation of drug-loaded nanoparticles. The phase transition of the mixed system started at a slightly lower water fraction ($\varphi_{water} \sim 0.33$) than those of the pure *1.1*PNEM ($\varphi_{water} \sim 0.36$) and IMC ($\varphi_{water} \sim 0.42$) indicating that, besides the soluble–insoluble transition of PNIPAM, the decrease in the drug solubility has also a bearing on the process of micellization and loading of the double-hydrophilic copolymer. Because of the cononsolvency of PNIPAM, the self-association of PNIPAM-*g*-PEO promoted the IMC incorporation into the formed micellar associates. Since they remained physically stable upon further addition of water one can presume that the encapsulation of a relatively high amount of drug and the arising drug–polymer attractive forces reinforced the micellar structure and enhanced its resistance against dissociation. In DMF–water solution (Fig. 5b), the cononsolvent effect on the *1.1*PNEM-IMC mixture was similar to that of the pure copolymer. Due to the high solubility of IMC and PNIPAM-*g*-PEO in DMF, the phase separation region was limited to a narrow range of DMF–water ratios ($0.32 < \varphi_{water} < 0.45$) and the process was reversible. However, at $\varphi_{water} > 0.70$, far beyond the cononsolvent region of the copolymer, a second, irreversible phase transition was detected in the transmittance curve of *1.1*PNEM-IMC mixture which corresponded to the precipitation of the pure IMC. One can assume that PNIPAM-drug specific interactions dominate at this critical solution composition and might induce nanoparticles formation.

The appearance of irreversible phase transitions in the presence of IMC at 20 °C suggests that the process of IMC incorporation into the PNIPAM-*g*-PEO core–shell nanoparticles can be conducted at room temperature using loading procedures with the organic

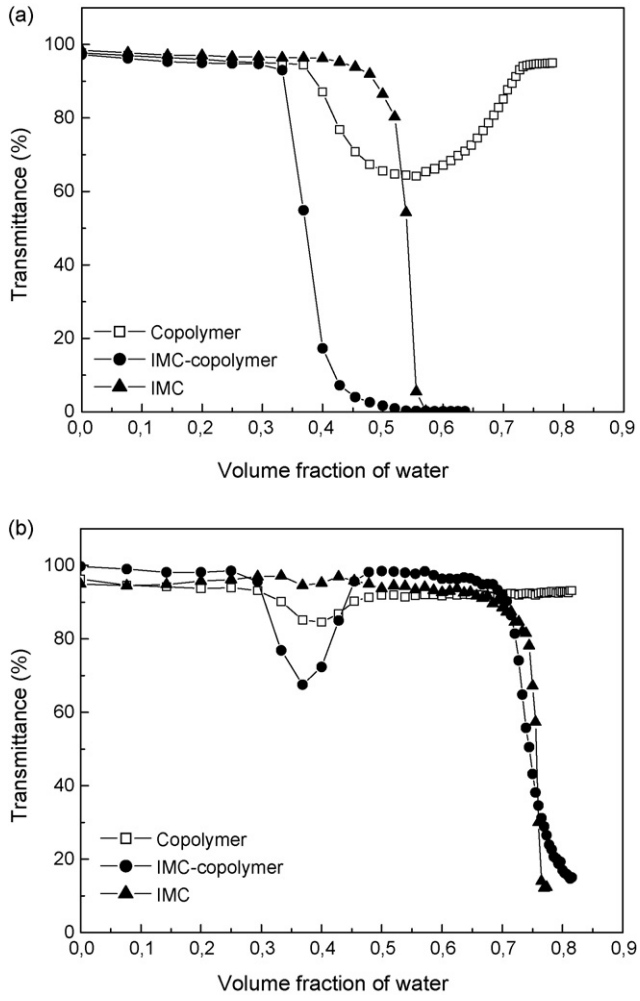

Fig. 5. Optical transmittance of mixed organic solvent–water solutions of *1.1*PNEM graft copolymer, of a *1.1*PNEM-IMC mixture at a 1:1 (w/w) ratio, and of IMC as a function of the volume fraction of water, at 20 °C. (a) Ethanol–water and (b) DMF–water solutions.

solvents tested. To obtain a deeper insight into the possible interactions between IMC and the copolymer and the mechanisms of IMC encapsulation in the dispersing media tested, IR и ^{1}H NMR spectroscopy studies were carried out.

3.2.3. IR studies of the interactions between IMC and PNIPAM-g-PEO copolymers

Fig. 6 shows IR spectra recorded on *1.1*PNEM graft copolymer and a blend of IMC and *1.1*PNEM at a feed weight ratio of 1:1 (w/w). The graft copolymer displayed absorption bands at 3432 cm^{-1} (free N–H vibration), 3279 cm^{-1} (hydrogen bonded N–H stretching), 1646 cm^{-1} (C═O stretching, amide I band) and 1547 cm^{-1} (N–H bending, amide II band) (Fig. 6a). IMC, deposited on KBr by evaporation of its ethanol solution, displayed characteristic carbonyl peaks at 1713 cm^{-1} and 1680 cm^{-1} (Fig. 6b). The spectrum of IMC-PNIPAM-*g*-PEO copolymer blend shows a difference in the shape and frequency of the observed absorption bands in comparison to the pure drug and the copolymer. In the N–H stretching region the absorption at 3432 cm^{-1} disappeared and a new peak at about 3336 cm^{-1} occurred (Fig. 6c). The results suggest that the absorptions at 3336 and 3280 cm^{-1} can be assigned to N–H stretching of different species: (i) N–H group hydrogen bonded to IMC carboxyl group, and (ii) N–H group hydrogen bonded to the carbonyl group of another amide function (Maeda et al., 2000; Zhang et al., 2007). Obviously, the proton donor ability of the OH bond of the IMC car-

boxylic group is higher than that of the N–H bond. Furthermore, the interactions between IMC and *1.1*PNEM also resulted in changes in the C=O stretching region. The shoulder detected at 1622 cm^{-1} can be interpreted as arising from the amide carbonyl hydrogen bonded with the carboxylic acid group of IMC. The decrease in the frequency of the amide I band indicates a stronger hydrogen bonded state at the carbonyl group in the IMC-PNIPAM-*g*-PEO blend than that in the parent graft copolymer.

3.2.4. Structure of IMC-loaded PNIPAM-g-PEO nanoparticles in aqueous solution studied by ^1H NMR

The NMR technique is a valuable tool to gain information about core–shell structures. The signals assigned to solvated coronal chains should be clearly seen in the NMR spectrum, while the ones corresponding to the desolvated chains forming the core of the micelles should decrease and even vanish.

The ^1H NMR spectra of IMC in NaOD/D_2O, of *0.3*PNEM graft copolymer in D_2O and of the D_2O dispersion of IMC/*0.3*PNEM nanoparticles prepared by dialysis from DMF at a 1:1 (w/w) drug-to-polymer ratio are presented in Fig. 7. All spectra were recorded at 20 °C. The spectrum of *0.3*PNEM graft copolymer (Fig. 7b) shows characteristic signals due to the PEO side chains at δ 3.67 (oxyethylene protons, H3) and the PNIPAM main chain at δ 3.86 methine (H1) and at δ 1.1 methyl (H2) protons of the pendent isopropyl groups. The ratio of the integrated peak intensity of the methyl

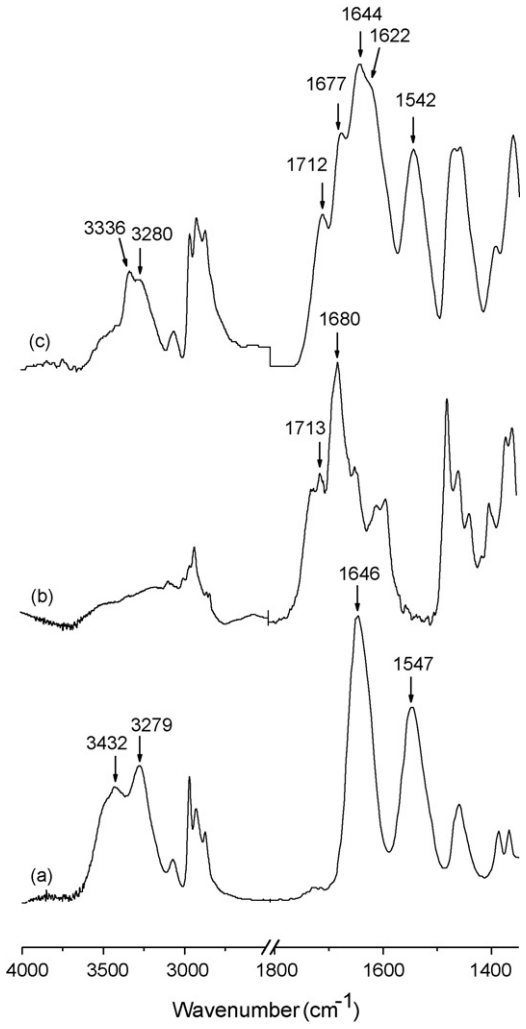

Fig. 6. Infrared spectra of (a) *1.1*PNEM graft copolymer, of (b) IMC and of (c) *1.1*PNEM-IMC blend at a 1:1 (w/w) ratio.

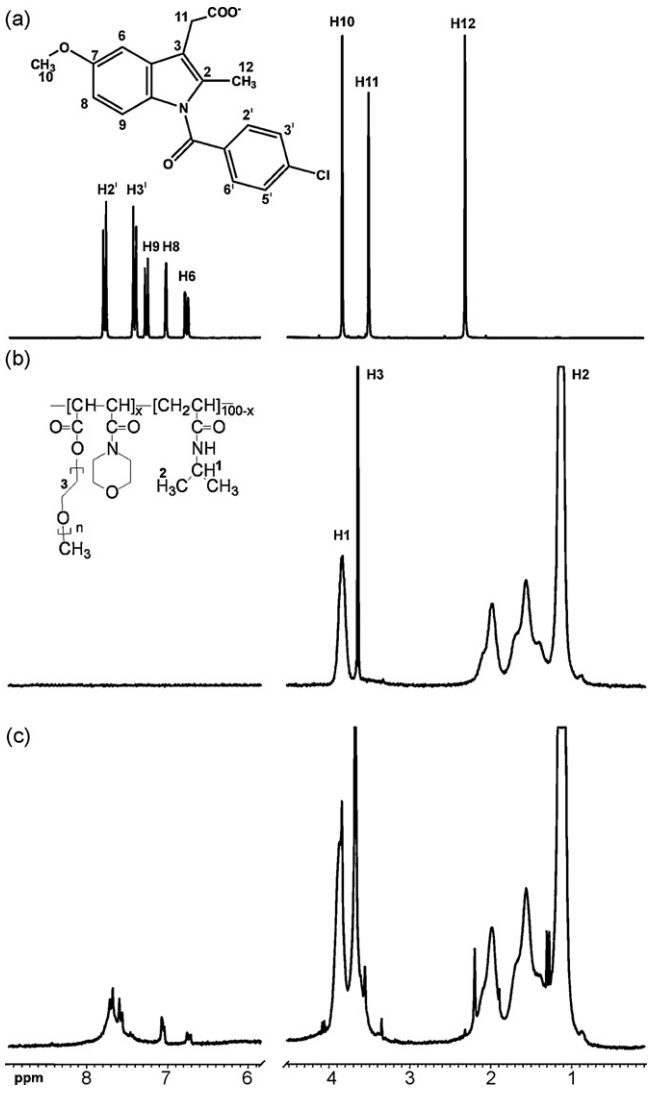

Fig. 7. ^1H NMR spectra of (a) IMC in NaOD/D_2O, of (b) *0.3*PNEM graft copolymer in D_2O and of (c) IMC/*0.3*PNEM nanoparticles in D_2O, at 20 °C.

protons of the isopropyl groups to that of the oxyethylene protons was 10.86. In the spectrum of the IMC-loaded nanoparticles (Fig. 7c), the same ratio was equal to 6.7, quite lower than that of the parent graft copolymer. This indicates that some isopropyl groups from the PNIPAM backbone are entrapped in the nanoparticles core where they loose their mobility, while others are sufficiently mobile to be observed in the ^1H NMR spectrum. One can suppose that a fraction of PNIPAM segments remains partially solvated, while another is involved in interactions with IMC. In ^1H NMR analysis, hydrogen-bonding and hydrophobic interactions of IMC with polymer molecules can be accounted by the change in the chemical shifts ($\Delta\delta = \delta_{nanoparticle} - \delta_{IMC}$) (Iohara et al., 2008). As can be seen in Table 2, most protons of the hydrophobic parts of IMC displayed relatively large changes in their chemical shifts in the IMC-loaded nanoparticle, namely about 0.21 ppm for H3′, H5′ in the p-chlorobenzoyl ring, 0.25 ppm and 0.08 ppm for H6 and H9 in the six-membered ring of the indole moiety, and 0.08 ppm and 0.1 ppm for H10 and H11 in the OCH_3 and CH_2 groups, respectively, indicating intermolecular interactions between IMC and the hydrophobic parts of the PNIPAM chain. Since the association of a hydrophobic drug with PNIPAM results in an increase in the hydrophobic character of the polymer (Coughlan and Corrigan, 2006), these interactions seem to make a major contribution to

Table 2
^{1}H chemical shifts (δ) of IMC and $\Delta\delta$ values for IMC/*0.3*PNEM nanoparticles prepared by dialysis from DMF at a 1:1 (w/w) ratio.

Position	IMC		IMC/*0.3*PNEM nanoparticles
	δ (ppm)	m, *J* (Hz)	$\Delta\delta$ (ppm)[a]
H2′, H6′	7.59	d, 7.0	−0.02
H3′, H5′	7.23	d, 7.0	0.21
H6	6.84	s	0.08
H8	6.58	d, 7.0	0.01
H9	7.15	d, 7.0	−0.25
H10	3.64	s	0.08
H11	3.32	s	0.10

[a] $\Delta\delta = \delta_{(IMC/0.3PNEM)} - \delta_{(IMC)}$.

the formation of IMC/PNEM nanoparticles in the DMF–water mixed solutions.

3.3. Characteristics and physical stability of IMC-loaded PNIPAM-g-PEO nanoparticles

The characteristics of IMC/*1.1*PNEM nanoparticles prepared by the dialysis and nanoprecipitation methods using ethanol and DMF as organic solvents are summarized in Table 3. The IMC-to-copolymer feed weight ratio significantly influences the drug loading content and entrapment efficiency in the nanoparticles, irrespective of the solvents employed. The quantity of encapsulated IMC (24–36%, w/w$_p$) and the entrapment efficiency (58–80%) were relatively low at the IMC-to-polymer ratio of 0.5:1, which was probably due to the insufficient amount of IMC in the system that should promote the formation of the micellar structure during the process of drug incorporation. However, the entrapment efficiency significantly increased at the IMC-to-polymer ratios of 0.75:1 and 1:1 (87–96%), reaching approximately 90% (w/w$_p$) encapsulation of the drug. Despite the large drug loading, these nanoparticles were systemically smaller than those prepared at the ratio of 0.5:1. They also retained a regular spherical shape as can be seen from the SEM images (Fig. 8) and did not display any morphology transitions (e.g., from spheres to cylinders) that often accompanied micelles formation and loading with such a high amount of drug (Giacomelli et al., 2007a,b).

Depending on the organic solvent and the drug-to-polymer ratio, the mean size of the particles prepared by the dialysis method varied in the range of 300–600 nm and exhibited high polydispersity, which indicates the existence of enhanced intermicellar association. Probably, due to the relatively lower flexibility of the branched copolymer structure and the slow solvent exchange, the collapse of the PNIPAM core was not sufficiently fast to prevent secondary aggregation. The type of the organic solvent strongly affected the nanoparticles size. The dialysis from DMF produced much larger particles than those obtained from ethanol. This agrees well with the IMC-*1.1*PNEM phase transition behavior observed in DMF–water mixed solutions. The contraction of *1.1*PNEM is much weaker in the absence of cononsolvency on PNIPAM, which leads to a poorer phase separation in the forming micellar structures. In contrast to the dialysis method, significantly smaller nanoparticles (<150 nm) with narrow size distribution were obtained by using the nanoprecipitation technique. The nanoprecipitation occurs by a rapid polymer desolvation as a result of complex and cumulated interfacial hydrodynamic phenomena (Fessi et al., 1989; Quintanar-Guerrero et al., 1998) that often enable the production of small-sized, homogeneous nanoparticles populations from a wide range of polymers, such as PLA, PLGA, PLGA-*b*-PEO, cellulose derivatives and poly(ε-caprolactone)-*b*-PEO (Thioune et al., 1995; Chorny et al., 2002; Vangeyte et al., 2004; Bilati et al., 2005; Cheng et al., 2007).

To test physical stability of the nanoparticles, aqueous dispersions of IMC/*2.2*PNEM nanoparticles were prepared by nanoprecipitation at 0.5:1, 0.75:1 and 1:1 IMC-to-polymer ratios; they were dialyzed against water and then stored at 20 °C for seven days (Table 4). For all samples studied, the ratios of the particle size after storage to its initial size were in the range of 1.0 ± 0.1, indicating that the nanoparticles remained intact and colloidally stable (Lin et al., 2003). In addition, it was found that each system maintained its drug loading content at the end of the study, regardless of

Table 3
Characteristics of IMC/*1.1*PNEM nanoparticles prepared by the dialysis and nanoprecipitation methods.

IMC/graft copolymer (w/w) ratio	Solvent	Method	IMC loading (w/w$_p$%)	EE (%)	Mean particle size (nm)[a]	PD[b]
1:1	DMF	Dialysis	88.68	94	478.9 ± 16.9	0.638 ± 0.104
0.75:1	DMF	Dialysis	68.14	95	526.3 ± 24.6	0.691 ± 0.152
0.5:1	DMF	Dialysis	28.70	66	593.3 ± 21.4	0.742 ± 0.204
1:1	Ethanol	Dialysis	83.34	92	288.4 ± 31.0	0.354 ± 0.211
0.75:1	Ethanol	Dialysis	67.72	90	317.6 ± 49.4	0.392 ± 0.108
0.5:1	Ethanol	Dialysis	23.72	58	362.2 ± 76.7	0.454 ± 0.047
1:1	Ethanol	Nanoprecipitation	78.89	87	87.3 ± 3.2	0.102 ± 0.026
0.75:1	Ethanol	Nanoprecipitation	64.04	87	129.1 ± 3.3	0.139 ± 0.026
0.5:1	Ethanol	Nanoprecipitation	35.98	80	146.5 ± 1.4	0.095 ± 0.020

[a] The average diameter of three independent measurements.
[b] Polydispersity.

Table 4
Stability of IMC/*2.2*PNEM nanoparticles in water at 20 °C.

IMC/*2.2*PNEM (w/w) ratio	Initial nanoparticles' characteristics			One day of storage			Seven days of storage		
	Particle size (nm)[a]	PD[b]	DLC (w/w$_p$%)[c]	Particle size ratio[d]	PD[b]	DLC (w/w$_p$%)[c]	Particle size ratio[d]	PD[b]	DLC (w/w$_p$%)[c]
1:1	106.2 ± 1.5	0.132 ± 0.022	84.86	1.04	0.164 ± 0.015	85.44	1.08	0.164 ± 0.013	84.32
0.75:1	124.6 ± 5.4	0.125 ± 0.025	67.14	1.06	0.152 ± 0.034	66.76	1.04	0.124 ± 0.018	66.61
0.5:1	140.2 ± 1.2	0.112 ± 0.027	41.40	0.99	0.110 ± 0.029	40.92	1.02	0.158 ± 0.034	42.12

[a] The average diameter of three independent measurements.
[b] Polydispersity.
[c] DLC was determined after filtering the dispersions through 1.2 μm membrane filter.
[d] Calculated as the ratio of the particle size after storage to its initial size.

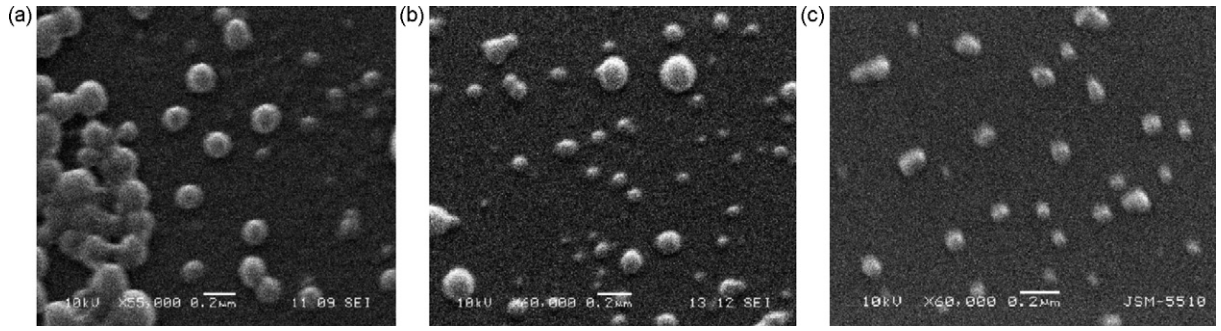

Fig. 8. SEM images of IMC-loaded *1.1*PNEM nanoparticles prepared by the dialysis or nanoprecipitation methods using ethanol as a cononsolvent. (a) Dialysis at a 1:1 feed weight ratio. (b) Dialysis at a 0.75:1 feed weight ratio. (c) Nanoprecipitation at a 1:1 feed weight ratio.

Table 5
Effect of temperature and PEO grafting degree on the size and size distribution of IMC-loaded nanoparticles prepared by nanoprecipitation from ethanol.

Polymer	IMC/graft copolymer (w/w) ratio	Temperature			
		20 °C		37 °C	
		Size (nm)[a]	PD[b]	Size (nm)[a]	PD[b]
*3.2*PNEM	1:1	75.3 ± 2.0	0.070 ± 0.020	75.2 ± 1.7	0.089 ± 0.033
*2.7*PNEM	1:1	98.8 ± 3.0	0.112 ± 0.021	90.9 ± 3.4	0.081 ± 0.076
*2.2*PNEM	1:1	101.1 ± 2.5	0.053 ± 0.041	104.7 ± 8.2	0.087 ± 0.040
*1.1*PNEM	1:1	87.3 ± 3.2	0.102 ± 0.026	89.7 ± 8.2	0.132 ± 0.040
*3.2*PNEM	0.5:1	94.3 ± 2.5	0.244 ± 0.069	91.3 ± 8.8	0.144 ± 0.042
*2.7*PNEM	0.5:1	123.9 ± 5.2	0.110 ± 0.055	100.6 ± 5.0	0.077 ± 0.009
*2.2*PNEM	0.5:1	138.4 ± 3.5	0.120 ± 0.010	115.4 ± 20.1	0.136 ± 0.030
*1.1*PNEM	0.5:1	146.5 ± 1.4	0.095 ± 0.020	118.0 ± 16.9	0.151 ± 0.004

[a] The average diameter of three independent measurements.
[b] Polydispersity.

the initial degree of drug encapsulation. These results imply that, in the range of the drug-to-polymer ratios used, the arising intramicellar physical interactions are sufficiently intensive and strong to confer thermodynamic and kinetic stability to the IMC-loaded PNIPAM-*g*-PEO core–shell structures at T < CPs of the copolymers.

3.4. Effect of temperature on the IMC-loaded PNIPAM-g-PEO nanoparticles

The change of the particle size and size distribution as a function of temperature was studied in nanoparticles dispersions whose molar content of PEO grafts ranged from 1.1 to 3.2 mol% (Table 5). The samples were prepared by nanoprecipitation at IMC-to-polymer ratios of 0.5:1 and 1:1 (w/w). The heating of the dispersions from 20 °C to 37 °C, did not influence the size of the particles obtained at the ratio of 1:1. The mean particle diameters were around 100 nm, regardless of the grafting degree and the temperature, indicating that the particles possessed quite compact structure. Presumably at the higher degree of drug encapsulation, the enhanced hydrogen-bonding and hydrophobic interactions between the molecules of IMC and PNIPAM allows the formation of a dense hydrophobic core at 20 °C that does not shrink further above the CPs of the copolymers. At the drug-to-polymer ratio of 0.5:1, a decrease in the particle size with increasing the mole fraction of the PEO chains was observed at both temperatures studied. In addition, the particles size was smaller at 37 °C than at 20 °C, which might be associated with additional dehydration of the micellar structure diminishing the free volume between the core forming chains. The larger water content and relatively looser structure of these nanoparticles are likely to increase IMC release rate.

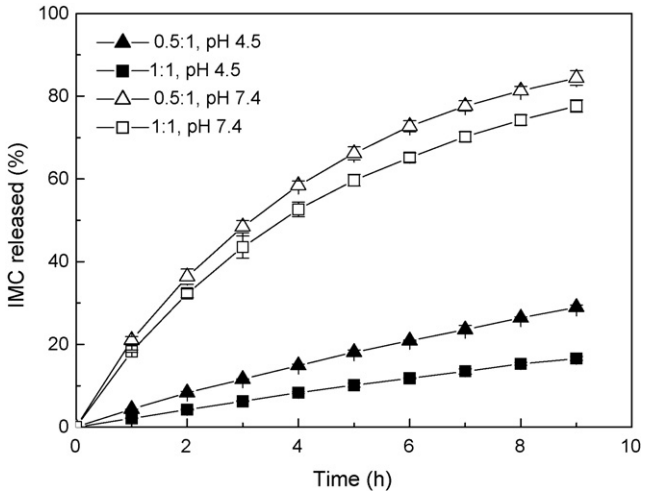

Fig. 9. IMC release profiles from IMC/*2.2*PNEM nanoparticles in pH 4.5 and pH 7.4 buffer solutions at 37 °C. Drug-to-polymer feed weight ratio: 0.5:1 or 1:1 (w/w); Mean values ± SD of 4 experiments.

3.5. Drug release behavior

The *in vitro* process of IMC release was examined in nanoparticles with different molar content of PEO grafts and drug loading. The experiments were carried out in pH 4.5 acetate buffer solution and pH 7.4 PBS using samples prepared by nanoprecipitation. The increase in the molar content of PEO from 1.2 to 3.2 mol% did not affect IMC release rate. For the samples with similar drug loading, no statistically significant difference ($p > 0.05$) was found between the release profiles in pH 4.5 acetate buffer solution and in pH 7.4 PBS (data not shown). Evidently at such a low molar content, the change in the PEO concentration is insufficient to regulate the release rate.

The amount of the encapsulated drug, however, significantly influenced the process of IMC release from IMC/PNEM

nanoparticles. Fig. 9 shows IMC release profiles of IMC/*2.2*PNEM nanoparticles obtained at 0.5:1 and 1:1 (w/w) drug-to-polymer ratios. In pH 4.5 acetate buffer solution, the process of IMC release was slower than in pH 7.4 PBS and showed a dependence on the loading degree of the micellar nanoparticles. After 9 h, the amount of released IMC was 28% and 16% for the IMC-to-polymer ratios of 0.5:1 and 1:1, respectively. The drug release rate at pH 4.5 was determined by both the low solubility of IMC in the dissolution medium and the presence of hydrogen-bonding and hydrophobic interactions between IMC and PNIPAM segments in the nanoparticles core. In pH 7.4 PBS, the quantity of IMC released from the nanoparticles over the tested period of 9 h reached 80%. There was a slight difference in the amount of released drug depending on the loading content. The pH-sensitivity of the hydrogen-bonding interactions between the carboxylic acid group of IMC and the amide groups of PNIPAM in the core have a bearing on the fast release rate. At pH 7.4, IMC is in a dissociated state, its solubility increases and the physical interactions within the micellar structure significantly weaken due to the disruption of the drug–polymer hydrogen bonding, which enhances the drug release rate.

4. Conclusions

Biocompatible thermally responsive double-hydrophilic PNIPAM-*g*-PEO copolymers containing 0.3–3.2 mol% PEO grafts were synthesized by copolymerizing MPEO phtalimido maleate with *N*-isopropylacrylamide in the presence of morpholine as an isomerization catalyst. PNIPAM-*g*-PEO core–shell nanoparticles were loaded with IMC by the dialysis and nanoprecipitation methods at room temperature, using DMF or ethanol as organic solvents. The addition of water to the organic solutions of pure PNIPAM-*g*-PEO or its mixture with indomethacin induced phase separation due to the cononsolvency of PNIPAM. In ethanol–water solutions, the phase transition of IMC and the pure copolymer occurred almost simultaneously at the tested concentrations, which promoted effective drug incorporation into the formed micellar structures. In DMF–water system, the formation of the nanoparticles did not correspond to the phase transition of the pure copolymer. In this case, the preparation of the nanoparticles was attributed to the IMC-PNIPAM hydrophobic interactions that were confirmed by ^{1}H NMR spectroscopy studies. The drug loading capacity of the nanoparticles depended on the drug-to-copolymer feed weight ratio, irrespective of the solvent or preparation method used. At a 0.5:1 IMC-to-polymer ratio, the loading content and entrapment efficiency of IMC were relatively low, but they significantly increased with the ratios of 0.75:1 and 1:1. The particle size and size distribution were affected by the different mechanisms of nanoparticles formation and the degree of loading under the applied preparation conditions. The nanoprecipitation method employing ethanol as a cononsolvent produced much smaller and narrow distributed nanoparticles than the dialysis from DMF. The prepared nanoparticles were stable in an aqueous solution and maintained their physical characteristics such as particle size and drug loading content during seven days of storage. It was demonstrated that the degree of *in vitro* IMC release from the PNIPAM-*g*-PEO nanoparticles in pH 7.4 PBS and in pH 4.5 acetate buffer depended on the degree of drug loading. The molar content of PEO in the copolymer molecule did not affect IMC release rate.

Acknowledgments

The support of this research by the National Science Fund, Bulgarian Ministry of Education and Science through Project X-1303 and by the Scientific Medical Council at the Medical University of Sofia, Grant 23/2005 is gratefully acknowledged. We also thank Wyatt Technology Corporation (Santa Barbara, CA, USA) for the generous loan of the DAWN-DSP/Optilab light scattering system.

References

Allen, C., Maysinger, D., Eisenberg, A., 1999. Nano-engineering block copolymer aggregates for drug delivery. Colloids Surf. B: Biointerfaces 16, 3–27.
Bae, Y., Kataoka, K., 2005. Polymer assembly. In: Kwon, G.S. (Ed.), Polymeric Drug Delivery Systems. Taylor & Francis Group, Boca-Raton.
Bilati, U., Allémann, E., Doelker, E., 2005. Development of a nanoprecipitation method intended for the entrapment of hydrophilic drugs into nanoparticles. Eur. J. Pharm. Sci. 24, 67–75.
Bisht, H.S., Wan, L., Mao, G., Oupicky, D., 2005. pH-controlled association of PEG-containing terpolymers of N-isopropylacrylamide and 1-vinylimidazole. Polymer 46, 7945–7952.
Boutris, C., Chatzi, E.G., Kiparissides, 1997. Characterization of the LCST behaviour of aqueous poly(N-isopropylacrylamide) solutions by thermal and cloud point techniques. Polymer 38, 2567–2570.
Bromberg, L., 2008. Polymeric micelles in oral chemotherapy. J. Control. Release 128, 99–112.
Causse, J., Lagerge, S., de Menorval, L.C., Faure, S., 2006. Micellar solubilization of tributylphosphate in aqueous solutions of Pluronic block copolymers Part. I. Effect of the copolymer structure and temperature on the phase behavior. J. Colloids Interface Sci. 300, 713–723.
Chaw, C.-S., Chooi, K.-W., Liu, X.-M., Tan, C.-W., Wang, L., Yang, Y.-Y., 2004. Thermally responsive core-shell nanoparticles self-assembled from cholesteryl end-capped and grafted polyacrylamides: drug incorporation and in vitro release. Biomaterials 25, 4297–4308.
Chen, H., Zhang, Q., Li, J., Ding, Y., Zhang, G., Wu, C., 2005. Formation of mesoglobular phase of PNIPAM-g-PEO copolymer with a high PEO content in dilute solutions. Macromolecules 38, 8045–8050.
Cheng, J., Teply, B.A., Sherifi, I., Sung, J., Luther, G., Gu, F.X., Levy-Nissenbaum, E., Radovic-Moreno, A.F., Langer, R., Farokhzad, O., 2007. Formulation of functionalized PLGA-PEG nanoparticles for in vivo target drug delivery. Biomaterials 28, 869–876.
Chorny, M., Fishbein, I., Danenberg, H.D., Golomb, G., 2002. Lipophilic drug loaded nanospheres prepared by nanoprecipitation: effect of formulation variables on size, drug recovery and release kinetics. J. Control. Release 83, 389–400.
Costa, R.O.R., Freitas, R.F.S., 2002. Phase behavior of poly(N-isopropylacrylamide) in binary aqueous solutions. Polymer 43, 5879–5885.
Coughlan, D.C., Quilty, F.P., Corrigan, O.I., 2004. Effect of drug physicochemical properties on swelling/deswelling kinetics and pulsatile drug release from thermoresponsive poly(N-isopropylacrylamide) hydrogels. J. Control. Release 98, 97–114.
Coughlan, D.C., Corrigan, O.I., 2006. Drug-polymer interactions and their effect on thermoresponsive poly(N-isopropylacrylamide) drug delivery systems. Int. J. Pharm. 313, 163–174.
Coughlan, D.C., Corrigan, O.I., 2008. Release kinetics of benzoic acid and its sodium salt from series of poly(N-isopropylacrylamide) matrices with various percentage crosslinking. J. Pharm. Sci. 97, 318–330.
Djordjevic, J., Barch, M., Uhrich, K.E., 2005. Polymeric micelles based on amphiphilic scorpion-like macromolecules: novel carriers for water-insoluble drugs. Pharm. Res. 22, 24–32.
D'Souza, S.S., DeLuca, P.P., 2006. Methods to assess *in vitro* drug release from injectable polymeric particulate systems. Pharm. Res. 23, 460–474.
Eeckman, F., Amighi, K., Moës, A.J., 2001. Effect of some physiological and non-physiological compounds on the phase transition temperature of thermoresponsive polymers intended for oral controlled-drug delivery. Int. J. Pharm. 222, 259–270.
Fessi, H., Puisieux, F., Devissaguet, J.-P., Ammoury, N., Benita, S., 1989. Nanocapsule formation by interfacial polymer depositin following solvent displacement. Int. J. Pharm. 55, R1–R4.
Gaucher, G., Dufresne, M.-H., Sant, V.P., Kang, N., Maysinger, D., Leroux, J.C., 2005. Block copolymer micelles: preparation, characterization and application in drug delivery. J. Control. Release 109, 169–188.
Giacomelli, C., Schmidt, V., Borsali, R., 2007a. Specific interactions improve the loading capacity of block copolymer micelles in aqueous media. Langmuir 23, 6947–6955.
Giacomelli, C., Schmidt, V., Borsali, R., 2007b. Nanocontainers formed by self-assembly of poly(ethylene oxide)-b-poly(glycerol monomethacrylate)-drug conjugates. Macromolecules 40, 2148–2157.
Iohara, D., Hirayama, F., Ishiguro, T., Arima, H., Uekama, K., 2008. Preparation of amorphous indomethacin from aqueous 2,6-di-O-methyl-β-cyclodextrin solution. Int. J. Pharm. 354, 70–76.
Kataoka, K., Harada, A., Nagasaki, Y., 2001. Block copolymer micelles for drug delivery: design, characterization and biological significance. Adv. Drug Deliv. Rev. 47, 113–131.
Konstantinov, S.M., Eibl, H., Berger, M.R., 1999. BCR-ABL influences the antileukaemic efficacy of alkylphosphocholines. Br. J. Haematol. 107, 365–380.
Lin, W.-J., Juang, L.-W., Lin, C.-C., 2003. Stability and release performance of a series of pegylated copolymeric micelles. Pharm. Res. 20, 668–673.
Liu, X.-M., Wang, L.S., Wang, L., Huang, J., He, C., 2004. The effect of salt and pH on the phase transition behaviors of temperature-sensitive copolymers based on N-isopropylacrylamide. Biomaterials 25, 5659–5666.

Lowe, T.L., Tenhu, H., 1998. Interactions of thermally responsive polyelectrolyte lattices with low molar mass organic molecules studied by light scattering. Macromolecules 31, 1590–1594.
Maeda, Y., Higuchi, T., Ikeda, I., 2000. Change in hydration state during the coil-globule transition of aqueous solutions of poly(*N*-isopropylacrylamide) as evidenced by FTIR spectroscopy. Langmuir 16, 7503–7509.
Mosmann, T., 1983. Rapid colorimetric assay for cellular growth and survival: application to proliferation and cytotoxicity assays. J. Immunol. Methods 65, 55–63.
Otsu, T., Ito, O., Toyoda, N., 1981. Polymers from alkyl maleates: further results of monomer-isomerization radical polymerization. Makromol. Chem., Rapid Commun. 2, 729–732.
Panayiotou, M., Garret-Flaudy, F., Freitag, R., 2004. Co-nonsolvency effects in the thermoprecipitation of oligomeric polyacrylamides from hydro-organic solutions. Polymer 45, 3055–3061.
Qiu, X., Wu, C., 1997. Study of core-shell nanoparticles formed through "coil-to-globule" transition of poly(N-isopropylacrylamide) grafted with poly(ethylene oxide). Macromolecules 30, 7921–7926.
Qiu, L.Y., Bae, Y.H., 2006. Polymer architecture and drug delivery. Pharm. Res. 23, 1–30.
Quintanar-Guerrero, D., Allémann, E., Fessi, H., Doelker, E., 1998. Preparation techniques and mechanisms of formation of biodegradable nanoparticles from preformed polymers. Drug Dev. Ind. Pharm. 24, 1113–1128.
Ranucci, E., Spagnoli, G., Sartore, L., Ferruti, P., Calicati, P., Schiavon, O., Veronese, F.M., 1994. Synthesis and molecular weight characterization of low molecular weight end-functionalized poly(4-acryloylmorpholine). Macromol. Chem. Phys. 195, 3469–3479.
Rao, J., Xu, J., Luo, S., Liu, S., 2007. Cononsolvency-induced micellization of pyrene end-labeled diblock copolymers of N-isopropylacrylamide and oligo(ethylene glycol) methyl ether methacrylate. Langmuir 23, 11857–11865.
Rijcken, C.J.F., Soga, O., Hennink, C.F., Van Nostrum, C.F., 2007. Triggered destabilisation of polymeric micelles and vesicles by changing polymer polarity: an attractive tool for drug delivery. J. Control. Release 120, 131–148.
Rösler, A., Vandermeulen, G.W.M., Klok, H.A., 2001. Advance drug delivery devices via self-assembly of amphiphilic block copolymers. Adv. Drug Deliv. Rev. 53, 95–108.
Schmaljohann, D., 2006. Thermo- and pH-responsive polymers in drug delivery. Adv. Drug Deliv. Rev. 58, 1655–1670.
Tanaka, F., Koga, T., Kojima, H., Winnik, F., 2009. Temperature- and tension induced coil-globule transition of poly(N-isopropylacrylamide) chains in water and mixed solvent of water/methanol. Macromolecules 42, 1321–1330.
Thioune, O., Fessi, H., Wouessidjewe, D., Devissaguet, J.-P., Puisieux, F., 1995. Hydroxypropylmethyl cellulose phthalate aqueous dispersion for coating: preparation by a nanoprecipitation method. STP Pharma Sci. 5, 367–372.
Torchilin, V.P., 2007. Micellar nanocarriers: pharmaceutical perspectives. Pharm. Res. 24, 1–16.
Vangeyte, P., Gautier, S., Jérôme, R., 2004. About the methods of preparation of poly(ethylene oxide)-b-poly(ε-caprolactone) nanoparticles in water. Analysis by dynamic light scattering. Colloids Surf. A: Physicochem. Eng. Aspects 242, 203–211.
Virtanen, J., Baron, C., Tenhu, H., 2000. Grafting of poly(N-isopropylacrylamide) with poly(ethylene oxide) under various reaction conditions. Macromolecules 33, 336–341.
Virtanen, J., Tenhu, H., 2000. Thermal properties of poly(N-isopropylacrylamide)-*g*-poly(ethylene oxide) in aqueous solutions: influence of the number and distribution of the grafts. Macromolecules 33, 5970–5975.
Virtanen, J., Lemmetyinen, H., Tenhu, H., 2001. Fluorescence and EPR studies on the collapse of poly(N-isopropylacrylamide)-*g*-poly(ethylene oxide) in water. Polymer 42, 9487–9493.
Winnik, F.M., Ottaviani, M.F., Boßmann, S.H., Pan, W., Garcia-Garibay, M., Turro, N.J., 1993. Cononsolvency of poly(N-isopropylacrylamide): a look at spin-labeled polymers in mixtures of water and tetrahydrofuran. Macromolecules 26, 4577–4585.
Wu, C., Qiu, X., 1998. Single chain core-shell nanostructure. Phys. Rev. Lett. 80, 620–622.
Zhang, J.X., Li, X.D., Yan, M.Q., Qui, L.Y., Jin, Y., Zhu, K.J., 2007. Hydrogen bonding-induced transformation of network aggregates into vesicles—a potential method for the preparation of composite vesicles. Macromol. Rapid Commun. 28, 710–717.
Zhu, P.W., Napper, D.H., 1996a. Volume phase transitions of poly(N-isopropylacrylamide) latex particles in mixed water-N,N-dimethylformamide solutions. Chem. Phys. Lett. 256, 51–56.
Zhu, P.W., Napper, D.H., 1996b. Coil-to-globule type transitions and swelling of poly(N-isopropylacrylamide) and poly(acrylamide) at latex interfaces in alcohol-water mixtures. J. Appl. Colloids Interface Sci. 177, 343–352.